

Evaluation of uptake and release of technetium-99m MIBI SPECT of pulmonary and mediastinal lesions

T. KOMORI, I. NARABAYASHI, R. MATSUI, Y. TATSU, K. SUEYOSHI,
I. ADACHI, T. SHIMIZU, R. NAMBA and Y. NAKATA

Department of Radiology, Osaka Medical College

We evaluated the uptake and release of Tc-99m MIBI in 7 benign and 30 malignant pulmonary and mediastinal lesions. Of the 37 patients, 13 underwent surgery; malignant involvement was examined in 21 mediastinal lymph nodes. Tl-201 SPECT was also performed in 10 patients. Tc-99m MIBI SPECT studies were performed on transverse SPECT images acquired 30 minutes and 3 hours after intravenous injection of 600 MBq of Tc-99m MIBI with three gamma camera detectors (GCA-9300A). Regions of interest were set in the area of abnormal uptake of Tc-99m MIBI and in an area of normal tissue in the contralateral lung. The uptake ratio of the lesion in the contralateral normal lung was obtained on the early image (early ratio; ER) as well as the delayed image (delayed ratio; DR). The benign lesions showed significantly lower ER (1.6 ± 0.3) and DR (1.4 ± 0.4) than the malignant lesions (1.9 ± 0.5 and 1.8 ± 0.5 , respectively; both $p < 0.05$). There was no significant difference in the retention index (RI), calculated as $RI = (DR - ER)/ER \times 100$. The DR obtained with Tl-201 SPECT images was significantly higher than that obtained with Tc-99m MIBI SPECT ($p < 0.05$). For the detection of mediastinal lymph node metastases, the early images showed sensitivity, specificity, and accuracy of 85.7%, 100%, and 95.2%, respectively, for the delayed images these values were 85.7%, 92.9%, and 90.5%, respectively. These results suggest that the uptake ratio of Tc-99m MIBI is a useful index in assessing benign or malignant pulmonary and mediastinal lesions.

Key words: technetium-99m MIBI, lung cancer, single photon emission computed tomography (SPECT), thallium-201

INTRODUCTION

TECHNETIUM-99m hexakis-2-methoxyisobutylisonitrile (Tc-99m MIBI) was recently approved for use as a myocardial perfusion imaging agent.^{1,2} It is an isonitrile with myocardial distribution proportional to regional blood flow. Intracellularly, it is sequestered largely within the mitochondria.^{3–5} Although many reports^{6–10} described accumulation of Tc-99m MIBI in various kind of tumors, there have been few clinical evaluations that included the study of the washout of Tc-99m MIBI from the tumor. The objective of this study was to evaluate the uptake and

washout of Tc-99m MIBI in pulmonary and mediastinal lesions and mediastinal lymph nodes in patients with lung cancer.

MATERIALS AND METHODS

We studied a total of 37 patients with pulmonary and mediastinal lesions at our institution (Table 1). The group studied included 24 men and 13 women (age range, 42–79 yr; mean age, 62 yr). Informed consent was obtained from every patient. The histologic diagnosis was obtained by biopsy or by surgery in all the patients except 4 with pulmonary tuberculosis. Thirty minutes and 3 hours after intravenous injection of 600 MBq of Tc-99m MIBI, pulmonary single photon emission computed tomography (SPECT) images were acquired with a triple-head rotating gamma camera (GCA-9300A/HG, Toshiba). Ninety

Received October 4, 1996, revision accepted June 25, 1997.
For reprint contact: Tsuyoshi Komori, M.D., Department of Radiology, Osaka Medical College, 2–7, Daigaku-cho, Takatsuki, Osaka 569, JAPAN.

Table 1 Summary of the histological diagnose for the patients

Primary lung cancer	27*
Squamous cell ca	11
Adeno ca	13
Small cell ca	1
Large cell ca	1
Undifferentiated ca	1
Metastatic lung cancer**	1
Mediastinal lymphoma	1
Thymic cancer	1
Malignant lesion	30
Pulmonary tuberculoma	4
Sclerosing hemangioma	1
Thymoma	1
Post pneumonial scar	1
Benign lesion	7
Total	37

*: Thirteen patients underwent surgical operation and malignant involvement was examined in 21 mediastinal lymph nodes. Tl-201 SPECT was also performed in 10 of the 37 patients.

** : primary lesion is hepatocellular carcinoma.

ca: carcinoma

projections were obtained at 30 sec/view through a 360° rotation in a 128 × 128 matrix. Transverse, coronal and sagittal images were reconstructed with a slice thickness of 3.2 mm. We compared the axial SPECT image with CT and confirmed each slice which showed tumor accumulation. Irregular shaped ROI were outlined on the tumor region of the axial slice which was superimposed on these slices, and mean count of this ROI (count/pixel) was defined as tumor uptake. An ROI of the same shape and dimensions was also set in a region with normal tissue of the contralateral lung on the superimposed axial section of the early scans. The same method was applied in the delayed imaging with the same ROI. The uptake ratios of tumor-to-normal tissues were calculated on the early image (early ratio; ER) and on the delayed image (delayed ratio; DR). As normal tissues, contralateral normal lung tissue was chosen for lung tumors, and the normal lung tissue near the mediastinum for mediastinal lymph nodes. The retention index (RI) was calculated as follows:

$$RI = (DR - ER) / ER \times 100.$$

Tl-201 SPECT was also performed in 10 patients, and the images were compared with the Tc-99m MIBI SPECT images. Statistical analysis was performed by Student's t-test or Welch's t-test for unpaired data. We considered that a result was significant when the p value was less than 0.05.

The mediastinal lymph nodes of 13 patients who underwent thoracotomy for lung cancer were examined. When the uptake of the radiotracer in a mediastinal or hilar lymph node was clearly demonstrated, then it was interpreted as positive for metastasis. When the mediastinal

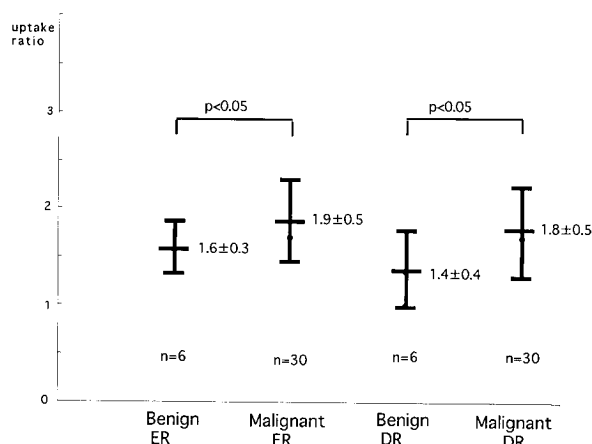


Fig. 1A Early ratio (ER) and delayed ratio (DR) in benign and malignant lesions. The error bar indicates the mean ± standard deviation.

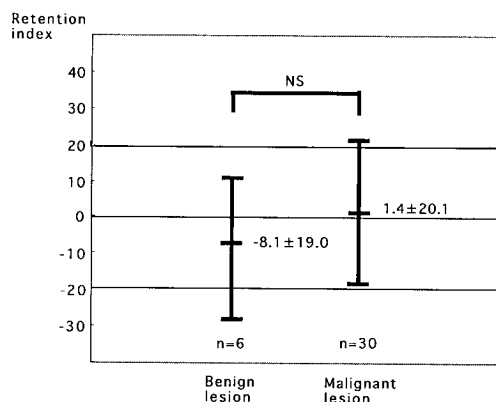


Fig. 1B Retention index (RI) in benign and malignant lesions. NS: not significant

and hilar uptake was equal to or less than that in the background, it was interpreted as negative for metastasis. The anatomical location of each area of abnormal uptake was determined in comparison with the CT and surgical findings and the numbering of lymph nodes was according to the lymph node mapping of the Japan Lung Cancer Society.¹¹ Malignant involvement of the mediastinal lymph nodes was confirmed by surgical operation and pathological study of the resected lymph nodes. The pathological classification for lung cancer was carried out according to the UICC TNM classification.¹²

RESULTS

1) Visual evaluation of Tc-99m MIBI SPECT images

In all patients with malignant lesions, Tc-99m MIBI accumulated in the lesion on the early images. On the early images, we could easily recognize the mediastinal lymph nodes because the major vascular structures were shown as the cold areas. The smallest malignant pulmonary lesion in this study, a 15 × 10 mm squamous cell

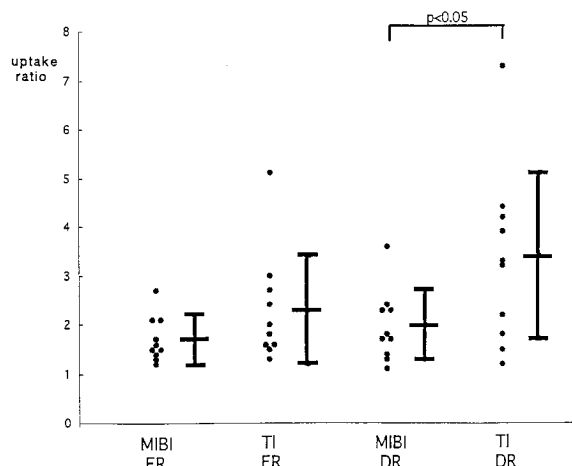


Fig. 2 Comparison of ER and DR values obtained from Tc-99m MIBI and Tl-201 SPECT images in primary lung cancers.

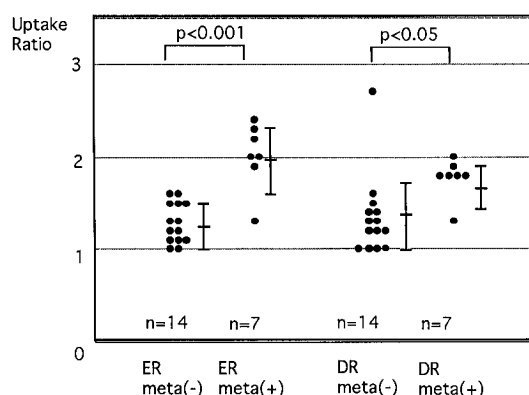


Fig. 3 Scatter plots of ER and DR of hilar and mediastinal lymph nodes in primary lung cancer patients.

carcinoma, was clearly demonstrated on the early scan. The squamous cell carcinomas tended to show washout of the activity on the delayed images, while adenocarcinomas did not. The early images revealed Tc-99m MIBI accumulation in all of the benign lesions except a thymoma which was a cystic tumor. All the benign lesions except pulmonary sclerosing hemangioma showed washout of the tracer on the delayed images.

2) Evaluation of ER, DR and RI

We evaluated the ER, DR and RI of the 30 malignant and 6 benign lesions. The patient with the thymoma was excluded from this evaluation, because the tumor did not show Tc-99m MIBI accumulation. The benign and malignant lesions showed significant differences in ER (1.6 ± 0.3 and 1.9 ± 0.5 , respectively; $p < 0.05$) and in DR (1.4 ± 0.4 and 1.8 ± 0.5 , respectively; $p < 0.05$) (Fig. 1A). There was no significant difference between the benign and malignant lesions in RI values (Fig. 1B).

3) Comparison of ER and DR values obtained from Tc-99m MIBI and from Tl-201 SPECT images

For 10 malignant lesions the ER values from Tc-99m MIBI were not significantly different from the ER values from Tl-201 images, but the DR from Tl-201 SPECT was significantly higher than that of Tc-99m MIBI SPECT images ($p < 0.05$) (Fig. 2).

4) Detection of mediastinal involvement with Tc-99m MIBI SPECT

By the quantitative method, the ER and DR of metastatic lymph nodes were found to be significantly higher than those of non-metastatic lymph nodes (Fig. 3). On early images when the cut-off level of ER was 1.6, the sensitivity, specificity and accuracy of Tc-99m MIBI SPECT were 85.7% (6/7), 100% (14/14) and 95.2% (20/21), respectively, and when the cut-off level of DR was 1.8, the sensitivity, specificity and accuracy were 85.7% (6/7), 92.9% (13/14) and 90.5% (19/21), respectively.

Two representative case reports, describing one patient each with and without demonstration of mediastinal metastasis, are presented below.

Case 1. The chest CT scan of a 61-year-old woman (Fig. 4A) revealed a coin shaped lesion (1.8 cm \times 1.2 cm) in the lower lobe of the right lung. The pretracheal lymph node (1.4 cm \times 1.0 cm) and the right hilar lymph node (1.3 cm \times 1.2 cm) were enlarged. The clinical stage was T2N2M0. Tc-99m MIBI SPECT demonstrated areas of abnormal accumulation corresponding to the pulmonary, mediastinal and hilar lesions on early scans (Fig. 4B), but the accumulation was slightly washed out on delayed scans (Fig. 4C). The ER and DR of the pretracheal lymph node were 1.3 and 1.4. The ER and DR of the right hilar lymph node were 1.4 and 1.5. The operative findings confirmed that an adenocarcinoma was present in the S⁶ segment of the right lung, and the pathological stage was T2N0M0. Neither the pretracheal nor the right hilar lymph nodes showed any cancer involvement.

Case 2. The chest CT scan of a 71-year-old woman (Fig. 5A) revealed a tumor shadow in the S¹⁺² segments of the left lung (1.5 cm \times 1.0 cm) and subaortic lymphadenopathy (2.2 cm \times 1.5 cm). The clinical stage was T1N2M0. Tc-99m MIBI SPECT demonstrated an abnormal accumulation corresponding to the pulmonary lesion and subaortic lymph node on both the early and delayed scans (Fig. 5B, C). The ER and DR of the subaortic lymph node were both 2.0. The operative findings confirmed the presence of an adenocarcinoma in the S¹⁺² segments of the left lung, and the pathological stage was T1N2M0.

DISCUSSION

Tc-99m MIBI, a relatively new imaging agent developed for the study of blood flow in the cardiac muscles, is known to be accumulated in various tumors.⁶⁻¹⁰ Its advantages are its low exposure dose, good image quality and

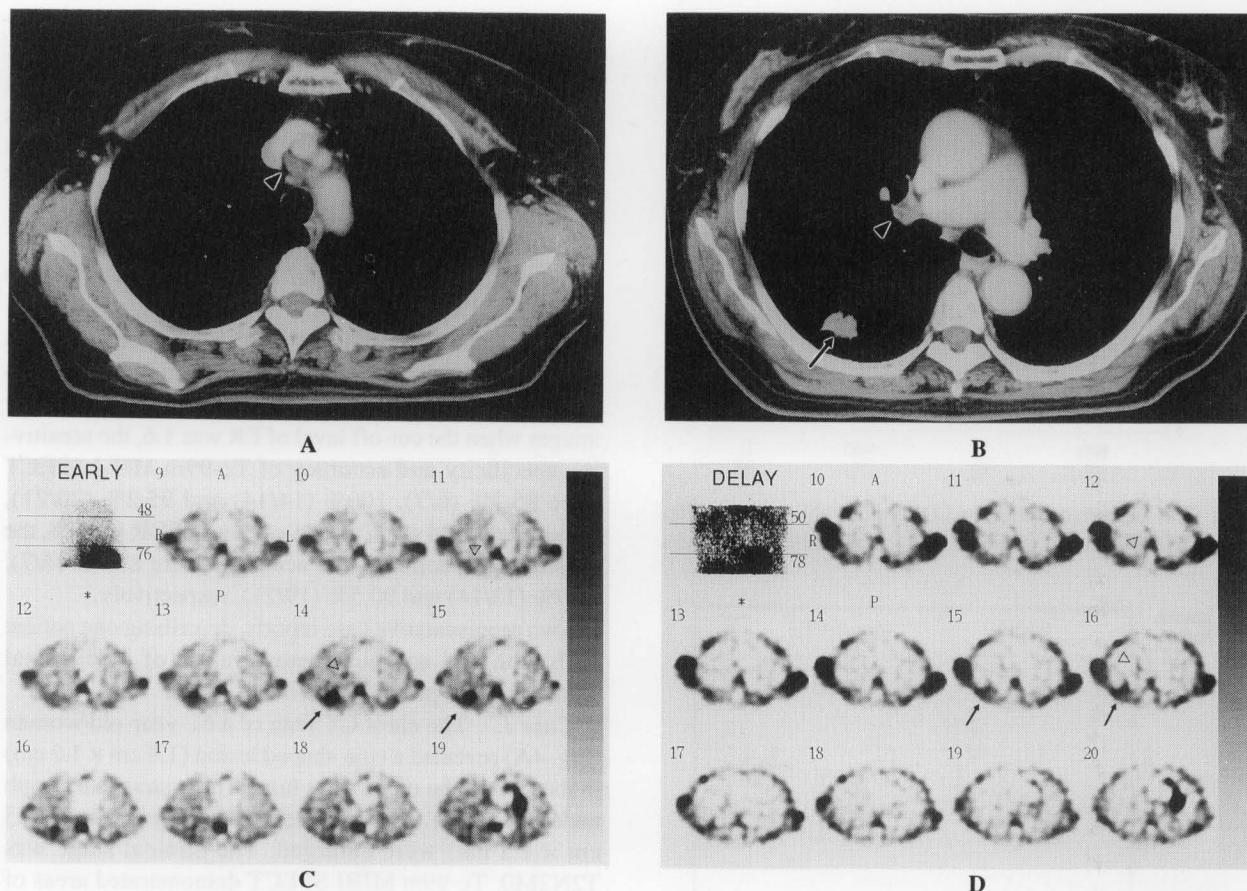


Fig. 4 A 61-year-old woman with adenocarcinoma at the right S⁶ (1.8 × 1.2 cm) and enlarged pretracheal and hilar lymph nodes (both, 1.4 × 1.0 cm) (pT2N0M0). Chest CT (A, B) discloses a solitary nodule in the right S⁶ (arrow) and enlarged pretracheal and hilar lymph nodes (arrowhead). Tc-99m MIBI early images (C) show abnormal accumulation at the tumor (arrow) and lymph nodes (arrowhead). On the delayed images (D) abnormal accumulation at the tumor (arrow) is seen, but the accumulation at the lymph nodes has been washed out.

clear SPECT images, and, like Tl-201, Tc-99m MIBI accumulates in various types of tumors, but there have been few clinical evaluations that included the study of the release of Tc-99m MIBI from the tumor. In this study of 37 patients with lesions in the pulmonary mediastinal space, a difference was noted between the uptake ratio of Tc-99m MIBI in benign tumors and that in malignant lesions, but there was no significant difference in their RI. Therefore, as a parameter for either benign or malignant lesions, the Tc-99m MIBI uptake ratio is considered more useful than the RI. This difference may arise from the differences between malignant and normal tissues in the number of mitochondria in cells and the amount of blood flow,^{13,14} but the exact reasons remain to be elucidated.

Hassan et al. serially examined the accumulation of Tc-99m MIBI in malignant tumors in the lung on planar images, and found that the accumulation of Tc-99m MIBI at 30 min was about 1.6-fold greater in the tumor than in the normal lung, while there was no difference in their time courses.⁶ Our *in vitro* examination with Hela cells revealed that Tl-201 was relatively slowly excreted from

cells of high malignancy, whereas Tc-99m MIBI was excreted at a constant rate from cells irrespective of their malignancy.¹⁵ These results indicate that the rate of wash-out of Tc-99m MIBI from cells is not related to their malignant potential. In the imaging of 10 malignant lesions by means of both Tl-201 and Tc-99m MIBI, the accumulation of Tl-201 was significantly greater than that of Tc-99m MIBI on the late images, suggesting that there exist different mechanisms of excretion of isotopes of Tl-201 and Tc-99m MIBI.

The presence or absence of the accumulation of Tc-99m MIBI in malignant tumors is generally considered useful in identifying multiple drug-resistant tumors, but since enzyme activities other than P-glycoprotein, such as glutathione S-transferase, are also involved in the drug-resistance of malignant tumors, it seems difficult to determine drug-resistance based solely on the presence or absence of the accumulation of Tc-99m MIBI.¹⁶ To test the validity of these generalizations clinically, it is necessary to evaluate the relationship between the degree of Tc-99m MIBI accumulation and the effects of chemotherapy.

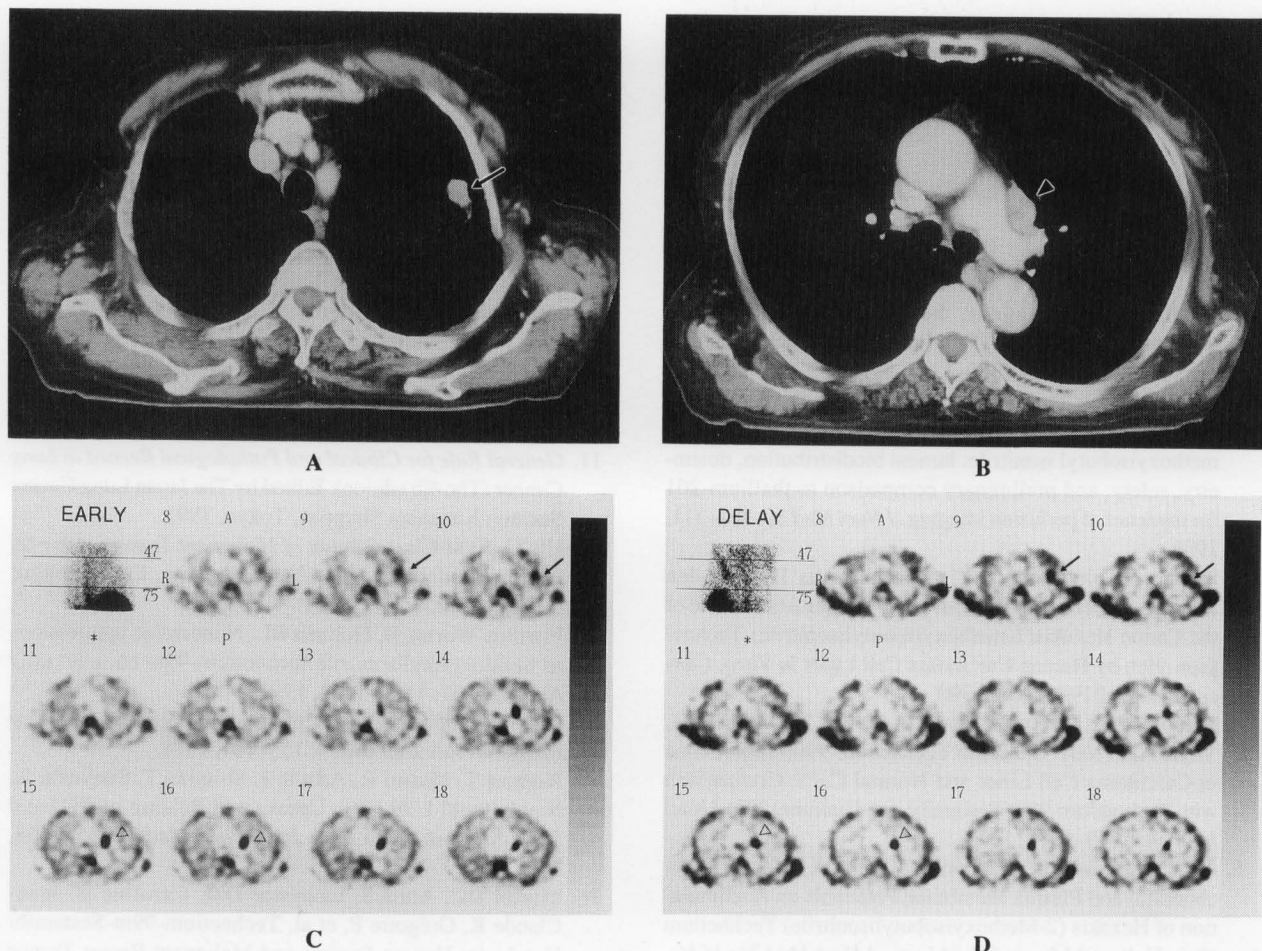


Fig. 5 A 71-year-old woman with adenocarcinoma at the left S¹⁺² (1.5 × 1.0 cm) and an enlarged subaortic arch lymph node (2.2 × 1.5 cm) (pT1N2M0). Chest CT (A, B) shows a solitary nodule in the left S¹⁺² (arrow) and an enlarged subaortic arch lymph node (arrowhead). Early transverse images of Tc-99m MIBI SPECT (C) abnormal uptake in the areas corresponding to the lesion (arrow) and subaortic arch lymph node (arrowhead). On the delayed images (D), the accumulation at the tumor (arrow) and subaortic arch lymph node (arrowhead) has not been washed out.

Based on our observations pointing to the usefulness of the uptake ratio of Tc-99m MIBI for the evaluation of tumor malignancy, we examined 21 lymph nodes in 13 patients with lung cancer who underwent surgery, and obtained high rates of accurate detection of 95.2% on the early images and 90.5% on the delayed images. Although only a small number of patients were examined, the results suggested that the uptake ratio of Tc-99m MIBI is useful for the diagnosis of metastasis to lymph nodes in patients with lung cancer. There were no differences between ER and DR for the diagnosis of metastasis to lymph nodes. Similarly, Chiti et al., with Tc-99m MIBI SPECT, examined the metastasis to lymph nodes in the mediastinal space in 36 patients with lung cancer postoperatively, and obtained accurate detection in 86% of the patients, as contrasted with only 64% of those examined by CT.¹⁷ In the 2 patients described in the case reports herein, metastases to the pretracheal lymph nodes and the lymph nodes in the right hilum of the lung were diagnosed

by CT before surgery, but in one of these patients the delayed Tc-99m MIBI SPECT images did not indicate Tc-99m MIBI accumulation, and no metastasis was found at surgery, indicating that in this patient the accumulation of Tc-99m MIBI was more useful than CT for the detection of metastasis. In the patient shown in Fig. 5 in whom metastasis to the subaortic lymph nodes was found at surgery, before surgery metastasis had been diagnosed from the size of the lymph nodes by CT, and also diagnosed by the accumulation of Tc-99m MIBI because its washout was slow. These results suggest that Tc-99m MIBI accumulation is at least equally as useful as CT for the diagnosis of metastasis to lymph nodes.

If our observation that the Tc-99m MIBI accumulation in malignant lesions is greater than in benign lesions is confirmed, it may be possible to establish a cut-off value as a parameter of malignancy following the accumulation of quantitative data for more patients.

In conclusion, it is suggested that the ratio of uptake of

Tc-99m MIBI is useful in differentiating between benign and malignant lesions in the pulmonary mediastinal space and for the diagnosis of metastasis to lymph nodes in the mediastinal space in patients with lung cancer.

REFERENCES

1. Holman BL, Jones AG, Lister-James L, Pavison A, Abrams MJ, Kirshenbaum JM, et al. A new Tc-99m-labeled myocardial imaging agent, hexakis(t-butylisonitrile) technetium(I) [Tc-99m TBI]: initial experience in the human. *J Nucl Med* 25: 1350–1355, 1984.
2. Wackers FJ Th, Berman DS, Maddahi J, Beller G, Fridrich R, Delaloye B, et al. Technetium-99m hexakis 2-methoxyisobutyl isonitrile: human biodistribution, dosimetry, safety, and preliminary comparison to thallium-201 for myocardial perfusion imaging. *J Nucl Med* 30: 301–311, 1989.
3. Delmon-Moingeon LI, Piwnica-Worms D, Van den Abbeele AD, Holman BL, Davison A, Jones AG. Uptake of the Cation Hexakis(2-methoxyisobutylisonitrile)-Technetium-99m by Human Carcinoma Cell Lines *In Vitro*. *Cancer Res* 50: 2198–2202, 1990.
4. Maublant JC, Zheng Z, Rapp M, Ollier M, Michelot J, Veyre A. *In Vitro* Uptake of Technetium-99m-Teboroxime in Carcinoma Cell Lines and Normal Cells: Comparison with Technetium-99m-Sestamibi and Thallium-201. *J Nucl Med* 34: 1949–1952, 1993.
5. Chiu ML, Kronauge JF, Piwnica-Worms D. Effect of Mitochondrial and Plasma Membrane Potentials on Accumulation of Hexakis (2-Methoxyisobutylisonitrile) Technetium (I) in Cultured Mouse Fibroblasts. *J Nucl Med* 31: 1646–1653, 1990.
6. Hassan IM, Sahweil A, Constantinides C, Mahmoud A, Nair M, Omar YT. Uptake and Kinetics of Tc-99m Hexakis 2-Methoxy Isobutyl Isonitrile in Benign and Malignant Lesions in the Lungs. *Clin Nucl Med* 14: 333–340, 1989.
7. Aktolun C, Bayhan H, Kir M. Clinical Experience with Tc-99m MIBI Imaging in Patients with Malignant Tumors: Preliminary Results and Comparison with Tl-201. *Clin Nucl Med* 17: 171–176, 1992.
8. Matsui R, Komori T, Narabayashi I, Namba R, Nakata Y, Tabuchi K, et al. Tc-99m Sestamibi Uptake by Malignant Lymphoma and Slow Washout. *Clin Nucl Med* 20: 352–356, 1995.
9. Kao CH, Wang SJ, Lin WY, Hsu CY, Liao SQ, Yeh SH. Differentiation of single solid lesions in the lungs by means of single-photon emission tomography with technetium-99m methoxyisobutylisonitrile. *Eur J Nucl Med* 20: 249–254, 1993.
10. Strouse PJ, Wang DC. Incidental Detection of Bronchogenic Carcinoma During Tc-99m SESTAMIBI Cardiac Imaging. *Clin Nucl Med* 18: 448–449, 1993.
11. *General Rule for Clinical and Pathological Record of Lung Cancer* (The 4th edition). Edited by The Japan Lung Cancer Society. Kanahara Shuppan, Tokyo, 1995.
12. UICC. *TNM Classification of Malignant Tumors*, 4th edn. Berlin, Heidelberg, New York, London, Paris, Tokyo: Springer, 1987.
13. Piwnica-Worms D, Holman BL. Noncardiac applications of hexakis(alkylisonitrile)technetium-99m complexes. *J Nucl Med* 31: 1166–1167, 1990.
14. Chen LB. Mitochondrial membrane potential in living cells. *Ann Rev Cell Biol* 4: 155–181, 1988.
15. Komori T, Matsui R, Adachi I, Shimizu T, Sueyoshi K, Narabayashi I. *In Vitro* Uptake and Release of ²⁰¹Tl and ^{99m}Tc-MIBI in HeLa Cell. *Jpn J Nucl Med* 32: 651–658, 1995.
16. Muriel DC, Anna S, Laurence DM, Caroline B, Jean-Claude K, Grégoire P, et al. Technetium-99m-Sestamibi Uptake by Human Benign and Malignant Breast Tumor Cells: Correlation with *mdr* Gene Expression. *J Nucl Med* 37: 286–289, 1996.
17. Arturo C, Lorenzo SM, Maurizio I, Giancomo G, Matteo I, Massimo DG, et al. Assessment of Mediastinal Involvement in Lung Cancer with Technetium-99m-Sestamibi SPECT. *J Nucl Med* 37: 938–942, 1996.